

Preparation, characterization and properties of novel 0–3 ferroelectric composites of $\text{Ba}_{0.95}\text{Ca}_{0.05}\text{Ti}_{0.8}\text{Zr}_{0.2}\text{O}_3$ –poly(vinylidene fluoride-trifluoroethylene)

E. El. Shafee*, S.M. Behery

Chemistry Department, Faculty of Science, Cairo University, 12613 Giza, Egypt

ARTICLE INFO

Article history:

Received 2 March 2011

Received in revised form 28 June 2011

Accepted 3 December 2011

Keywords:

Composite materials

Ceramics

Mechanical properties

Ferroelectricity

ABSTRACT

The present work describes the preparation and properties of a novel ceramic–polymer composites using $\text{Ba}_{0.95}\text{Ca}_{0.05}\text{Ti}_{0.8}\text{Zr}_{0.2}\text{O}_3$ (BCTZ) as a ceramic filler and poly(vinylidene fluoride trifluoroethylene) [P(VDF-TrFE)] as a polymer matrix. The BCTZ ceramics were prepared by the conventional solid-state reaction route whereas the BCZT–P(VDF-TrFE) composites with various BCTZ volume fractions were prepared by the combined method of solvent casting and hot pressing. The microstructure of the composites was investigated using scanning electron microscopy and X-ray diffraction. The dependences of the dielectric properties of the composites on BCTZ volume fraction was reported and analyzed in terms of the effective medium theory (EMT). The P – E hysteresis loops of the composites are strongly dependent on the ceramic volume fraction. The composites with higher ceramic volume fractions showed larger remanent polarization and smaller coercive field. The mechanical properties of the composites were investigated. Tensile strength showed enhancement at lower ceramic content and decreased with higher ceramic loading while Young's modulus showed increase with respect to the ceramic loading.

© 2011 Elsevier B.V. All rights reserved.

1. Introduction

In recent years, composites of ferroelectric polymers and ceramics have been widely used in underwater hydrophones, biomedical imaging with Ultrasound and non-destructive testing applications [1]. Ferroelectric polymer based 0–3 composite films are typically formed by suspending zero-dimensional ceramic powders into a three-dimensional continuative polymer matrix. The created composites combine the advantages of ceramics and polymers, presenting a novel type of material that is easy to process, and with high dielectric constant, high electromechanical efficiency, and high breakdown strength [2–6].

The ceramic fillers used in the composites are usually ferroelectrics with high dielectric constant, such as calcium or samarium and magnesium modified lead titanium [7–9], lead zirconate titanate [8,10], PMN-PT [5], and barium titanate (BaTiO_3) [6]. Among these fillers, BaTiO_3 is a very common piezoelectric material with high dielectric and electromechanical behavior, with the lead-free feature that is of special benefit from the viewpoint of environmental protection. The dielectric constant of BaTiO_3 is >10,000 at its Curie temperature (120 °C). However, when the temperature decreased from 120 °C to room temperature, the dielectric

constant of BaTiO_3 decreased sharply from above 10,000 to about 1100 because of the transfer of tetragonal phase of BaTiO_3 to cubic phase [11,12]. Therefore, in most cases, the BaTiO_3 –polymer composites have relatively low dielectric constants (usually <40) with BaTiO_3 volume fraction lower than 50 vol% [13–15]. In order to increase the dielectric constant of BaTiO_3 , barium calcium zirconate titanate $\text{Ba}_{0.95}\text{Ca}_{0.05}\text{Ti}_{0.8}\text{Zr}_{0.2}\text{O}_3$ (BCTZ) ceramic powders can be introduced to fabricated ceramic–polymer composite. BCTZ are commonly used as key materials for high capacitance multi-layer ceramic capacitors (MLCCs) with a temperature specification of Y5V and Ca and Zr are employed for broadening and shifting the dielectric maximum at the Curie point to room temperature [13,16]. Therefore, BCTZ has higher dielectric constant and more stable temperature coefficient of capacitance than BaTiO_3 .

Recently, there has been an increasing interest on using a ferroelectric polymer, such as poly(vinylidene fluoride) (PVDF), poly(vinylidene fluoride trifluoroethylene) [P(VDF-TrFE)], and poly(vinylidene fluoride trifluoroethylene-chlorofluoroethylene) [P(VDF-TrFE-CFE)] as a host material, because these polymers have a fairly low processing temperature and relatively high dielectric permittivity, which helps to raise the electrostriction of the composites [17–19]. Among these ferroelectric polymers, copolymers of P(VDF-TrFE) are the best known and exhibit the remarkable ferroelectric and piezoelectric performances [20–23]. Composites made of P(VDF-TrFE) and ferroelectric ceramics such as PZT and PMN-PT have been the subject of some research work [24–26], and

* Corresponding author. Tel.: +20 35676595; fax: +20 2 35727556.
E-mail address: ezeldain@gmail.com (E.El. Shafee).

detailed studies were reported on their dielectric, piezoelectric and pyroelectric properties [27–30]. It was shown that the dielectric constant increases with increasing ceramic volume fraction and that these composites have promising properties for applications in thermal imaging sensors and transducers [31].

The main goal of this research was to introduce a novel 0–3 type ceramic–polymer composite made of thermoplastic copolymer (P(VDF-TrFE)) with different loadings of ferroelectric, barium calcium zirconate titanate $\text{Ba}_{0.95}\text{Ca}_{0.05}\text{Ti}_{0.8}\text{Zr}_{0.2}\text{O}_3$ (BCTZ) ceramic. The microstructures obtained as well as the dielectric and ferroelectric properties and their dependencies on the BCTZ content are reported. Furthermore, the mechanical properties of these composites were also investigated.

2. Experimental details

The starting materials BaCO_3 (Aldrich, 99%), CaCO_3 (Aldrich 99.9%), TiO_2 (Aldrich 99.9%) and ZrO_2 (Aldrich, 99.9%) were weighed according to the stoichiometric composition $\text{Ba}_{0.95}\text{Ca}_{0.05}\text{Ti}_{0.8}\text{Zr}_{0.2}\text{O}_3$ (BCZT). The weighed powders were wet ball milled for 24 h using high-purity zirconia balls. After drying, calcinations was done in high-purity alumina crucible at 1200°C for 6 h in a conventional furnace. The calcined powder was again ball milled for about 24 h and then sieved. Thereafter, the powders were pressed into cylindrical pellets of diameter 10 mm and thickness of 1–2 mm using a hydraulic press at a pressure of $5 \times 10^7 \text{ N m}^{-2}$. Ploy(vinyl butyral (PVB) was used as a binder to reduce the brittleness of the pellets. The pellets were heated at 600°C for 1 h to burn out PVB binder and sintered at 1450°C for 2 h in air. Then, after crushing and grinding the sintered pellets, the ceramic powder was sieved through micosieve.

0–3 composites were prepared by solvent casting. The BCTZ powders were ultrasonically dispersed in methyl–ethyl–ketone (MEK) at the room temperature for 2 h in order to form a stable suspension. At the same time, the P(VDF-TrFE) copolymer with 70 mol% VDF (supplied by Piezotech) was also dissolved in MEK. Then the suspension of BCTZ in MEK was added to the PVDF-TrFE solution, the solution was magnetic stirred for 30 min, then subjected to ultrasonic treatment for another 30 min. The solution was heated to 80°C until it was almost dry and the composite was dried at 120°C overnight to ensure the complete evaporation of solvent. The bulk composite films were fabricated by hot pressing. The dried composite was cut into small pieces and then compression-molded between polyamide sheets at 200°C and 20 MPa. After taken of the polyamide sheets, the composite film thickness was ~ 1 mm. Composites with volume fraction of BCZT (ϕ_{cer}) ranging from 0.05 to 0.40 were fabricated. Prior measurements all composite films were annealed at 120°C for 2 h to increase the crystallinity of the copolymer.

Microstructure analyses were done using scanning electron microscopy (SEM, Jeol JSM-6400, Jeol Ltd., Japan) and X-ray diffraction spectrometry (XRD, Siemens D5000, Siemens AG, Germany), utilizing the JCPDS data file (International Center for Diffraction Data 1992, USA). For dielectric measurement, Aluminum electrodes were evaporated on the sides of the composite films to produce the desired capacitor structures. The dielectric properties of the samples were measured using a HP4191A impedance analyzer. Ferroelectric hysteresis loops were measured on a RT66A standard ferroelectric testing system at room temperature. Tensile properties of the composites were measured by a universal testing machine (Instron Universal Testing Machine Model 5544, Instron Co., USA). The tensile tests were performed at room temperature. At least five samples of each composite condition were tested to get a reliable result.

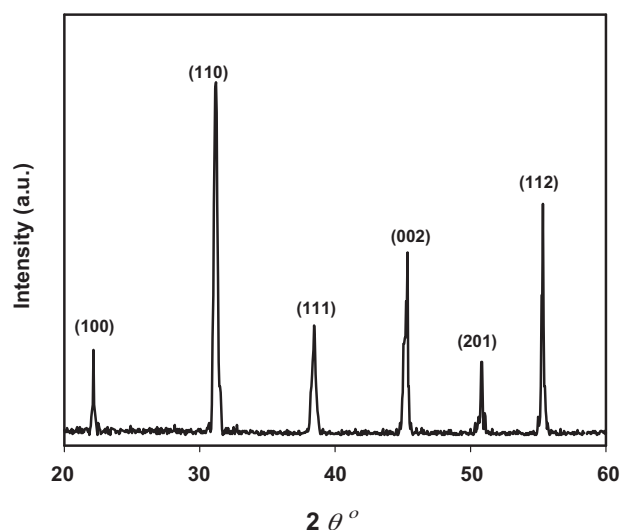


Fig. 1. X-ray diffraction patterns for the conventionally synthesized BCZT fillers.

3. Results and discussion

3.1. Microstructure

The phase purity of the BCZT ceramic filler was studied using powder X-ray diffraction technique. Fig. 1 shows the XRD patterns of the BCZT ceramics. A very strong XRD peaks with smaller full width at half maximum (FWHM) values are observed indicating better crystallinity. These peaks are attributed to the perovskite cubic phase of the BCZT. No evidence of the presence of secondary phases was found, neither reflection splitting nor super-lattice reflections were observed. The X-ray diffraction (XRD) patterns of pure P(VDFTrFE) and the BCZT/P(VDFTrFE) composites with different volume fractions are shown in Fig. 2. As is known, pure P(VDF-TrFE) with a VDF/TrFE molar ratio of 70/30 is a semicrystalline copolymer which consists of a ferroelectric crystalline β -phase embedded in an amorphous matrix, and the β -phase has a quasi-hexagonal close packing with orthorhombic $\text{mm}2$ structure [32]. As seen in Fig. 2, pure copolymer sample exhibits an intense

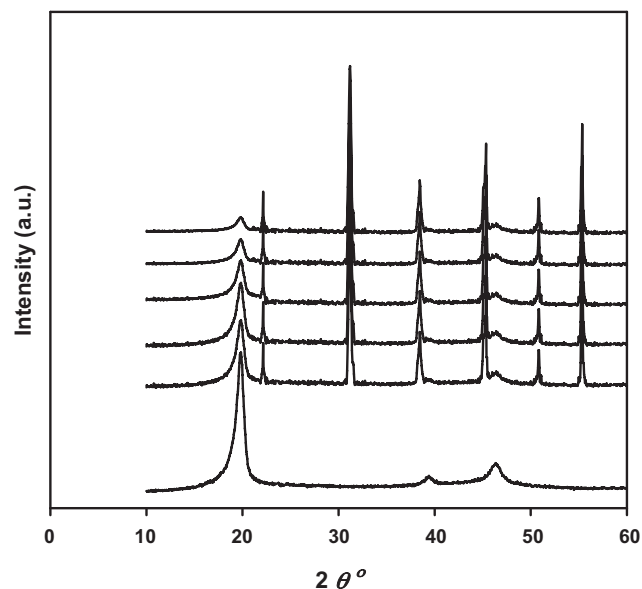


Fig. 2. X-ray diffraction patterns for BCZT/P(VDF-TrFE) composites with different ceramic volume fractions.

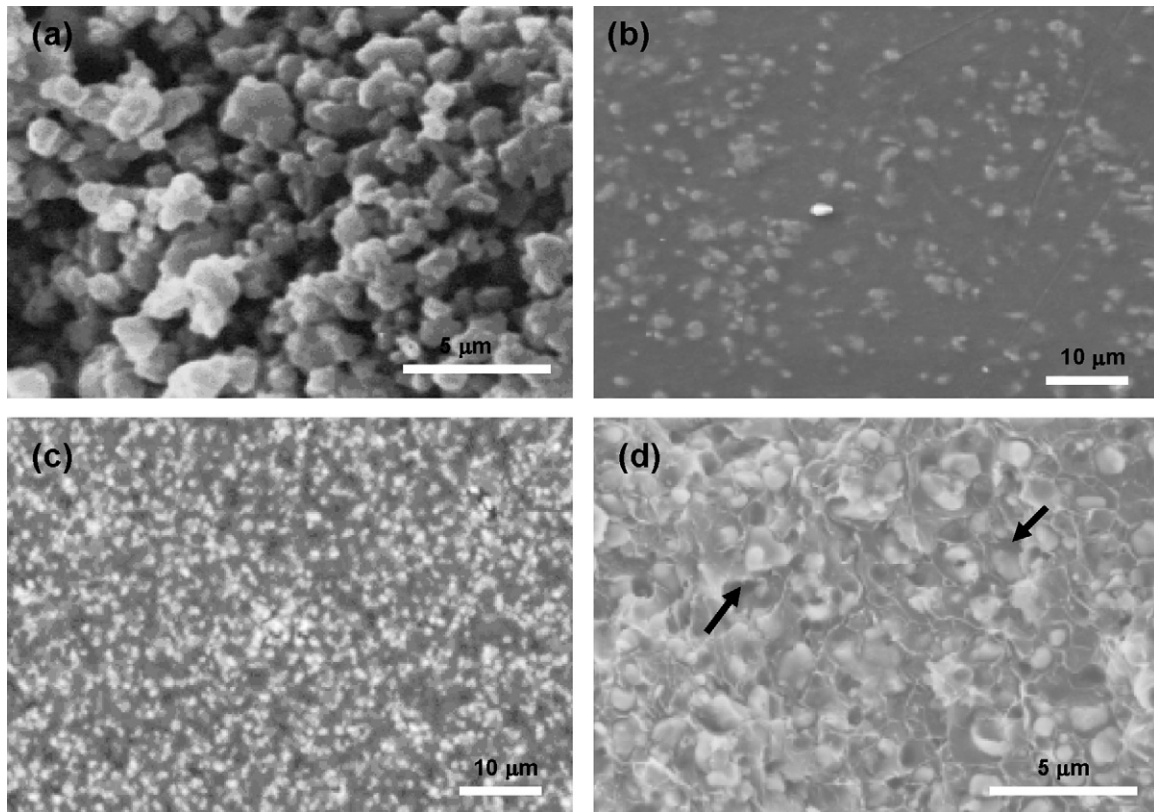


Fig. 3. SEM micrograph of BCZT powder and BCZT/P(VDF-TrFE) composites: (a) sieved BCZT particles, the specimen was prepared by spreading the powder onto an adhesive patch on the SEM stub, then applying a sputtered gold coating, (b and c) polished surface of the BCZT/P(VDF-TrFE) composites with $\phi_{cer} = 0.1$ and 0.3 , respectively, and (d) fractured surface of BCZT/P(VDF-TrFE) composite with $\phi_{cer} = 0.3$.

diffraction peak at $2\theta = 19.7^\circ$ which is a characteristic diffraction peak of the ferroelectric phase of P(VDF-TrFE) composed of the overlapping (110) and (200) reflections [33]. The XRD patterns of the composite samples consist of peaks belongs to both P(VDF-TrFE) copolymer and the BCZT perovskite ceramic powder. With increasing the ceramic content the intensity of the peaks for the ceramics increases. When the ceramic volume fraction reach 0.4, the (110) and (200) reflections of the copolymer becomes very weak due to the strong diffraction of the incorporated ceramic powders.

The morphologies of BCZT ceramic powdered and of the BCZT/P(VDF-TrFE) ceramic-polymer composites are observed by scanning electron microscopy (SEM) and the results are shown in Fig. 3. From Fig. 3a, the BCZT ceramic powder comprising of a well defined grains with an average grain size nearly between ~ 1 and $2 \mu\text{m}$. The surface morphologies of the composites are shown in Fig. 3b and c. The BCZT ceramic particles are uniformly distributed throughout the polymer, however a higher volume fraction of ceramic results in agglomeration in some localized regions thereby increases porosity. Fig. 3d shows the fractured surface of BCZT/P(VDF-TrFE) composite for 0.30 volume fraction of ceramic loading. The filler particles are seen to be clearly embedded in the polymer matrix and all the particles are neatly coated with P(VDF-TrFE), which establishes the (0–3) connectivity of the composites. Also some micropores are also visible in the morphology as indicated by the arrows.

3.2. Dielectric properties

The dielectric properties of the sintered BCZT ceramic were first investigated. Fig. 4 shows the dielectric constant as a function of temperature for BCZT ceramic, which was measured at

frequency of 1 kHz. As can be seen, two peaks are observed on the dielectric constant versus temperature curves in the measured temperature range between 20°C and 140°C . It is considered that these two peaks correspond to the polymorphic phase transitions from orthorhombic phase to tetragonal phase (T_{O-T}) and tetragonal phase to cubic phase (T_C), respectively [34]. The transition

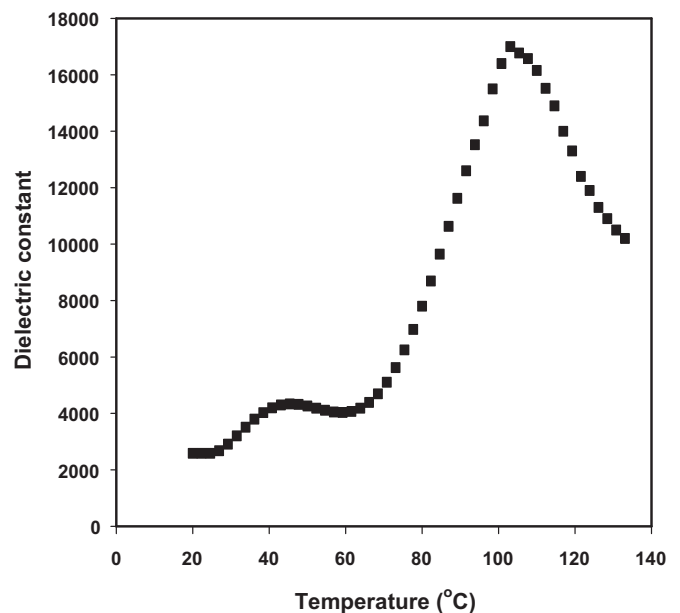


Fig. 4. Dielectric constant as a function of temperature for the sintered BCZT ceramics, measured at frequency of 1.0 kHz.

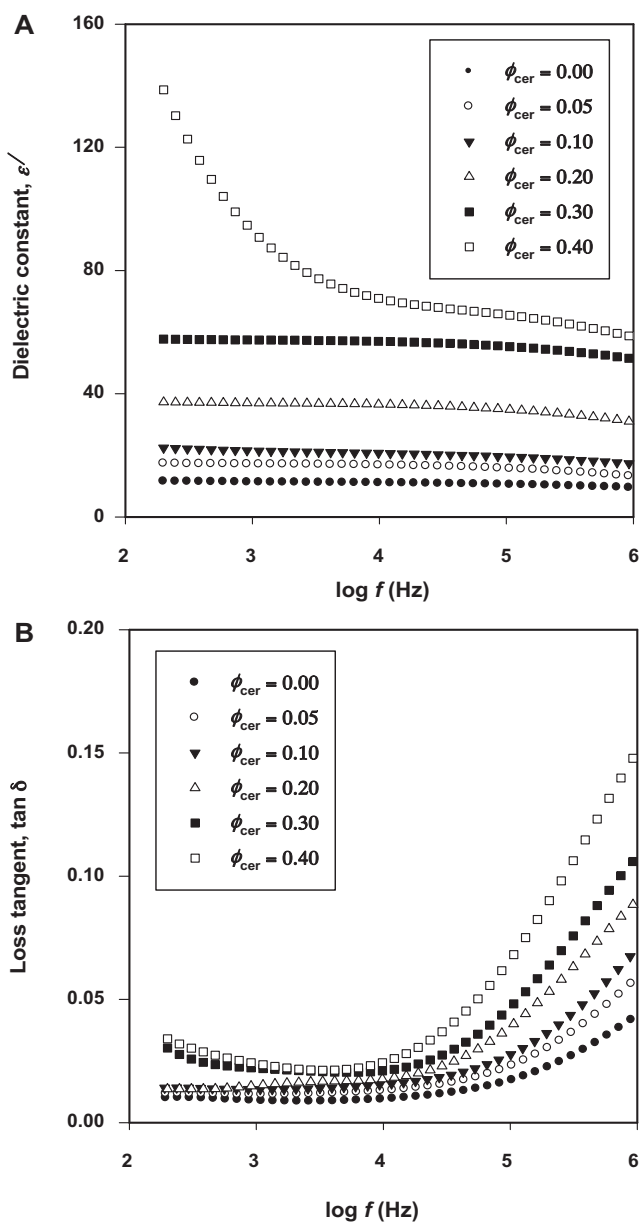


Fig. 5. The frequency dependence of the dielectric constant (ϵ') and dielectric loss tangent ($\tan \delta$) of BCTZ/P(VDF-TrFE) composites with various BCZT volume fractions.

temperatures of T_{0-T} and T_C are about 42°C and 107°C , respectively. The maximum value of the dielectric constant (ϵ'_{max}) at the Curie temperature, T_C , was found to be 15,000.

The frequency dependence of the dielectric constant (ϵ') and dielectric loss tangent ($\tan \delta$) of BCTZ/P(VDF-TrFE) composites were measured at room temperature as a function of the ceramic volume fraction, and the results are shown in Fig. 5. It can be seen that the dielectric properties change greatly with frequency. At low frequency (<1 kHz) the ϵ' and $\tan \delta$ in composites with more ceramic volume fraction reduce more quickly with frequency. This is mainly due to the contribution of the space charge which cannot be neglected in this low frequency range. Increasing the ceramic volume fractions induce more space charge which increase both the dielectric constant and loss at low frequency [35]. At high frequencies ϵ' decreases while the $\tan \delta$ decreases with frequency. This behavior is similar to that found in P(VDF-TrFE) and its composites with $(\text{Bi}_{0.5}\text{Na}_{0.5})_{0.94}\text{Ba}_{0.06}\text{TiO}_3$ [36]. These changes are mainly

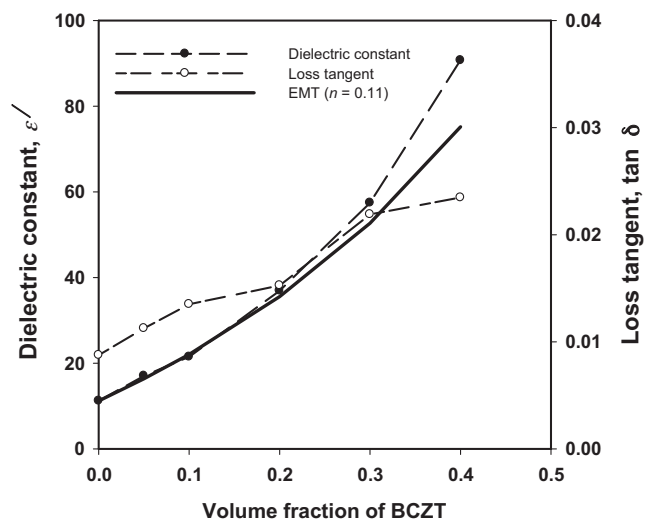


Fig. 6. Dielectric constant and loss tangent (1 kHz) of BCTZ/P(VDF-TrFE) composites at room temperature as a function of BCZT volume fractions. The close and open circles are the experimental data. The solid curve is calculated from the EMT model (see text).

caused by the dielectric relaxation in P(VDF-TrFE). It should be mentioned that the faster enhancement in $\tan \delta$ for composites with higher ceramic volume fraction in this high frequency range may be concerned with the rapid increase of conductivities with frequency in these composites.

The effect of increasing ceramic content on the dielectric constant and dielectric loss tangent of the composites at 1 kHz is shown in Fig. 6. As the ceramic content increases from 0 to 0.4 volume fraction, the dielectric constant increases from 11.2 to 90.7. The $\tan \delta$ of the composites at 1 kHz also increases with the amount of ceramic filler dispersed. This again may be attributed to the increase in the interfacial area between the BCZT and P(VDF-TrFE) which leads to an increase in the interfacial polarization and consequently higher dielectric loss.

The precise prediction of effective dielectric behavior of the composite from the relative dielectric constant of the components and the volume fraction of the filler is very important for the design of composites. Because the composites are statistical mixtures of two or more components, the relative dielectric constant is expected to be between the values of individual components. There have been several attempts to model and predict the effective properties of random filler distributed composites (see Ref. [37] and references cited in).

Recently, Rao et al. [38] proposed a model (Effective Medium Theory, EMT) to predict the dielectric permittivity of the composite in which the dielectric property of the composite is treated as an effective medium whose relative dielectric constant is obtained by averaging the dielectric constant values of the constituents. The EMT model is a self-consistent model that assumes a random unit cell consisting of each filler surrounded by a concentric matrix layer. The EMT model leads to the following equation to predict the effective dielectric constant of ceramic polymer composites.

$$\epsilon_{eff} = \epsilon_m \left[1 + \frac{\phi(\epsilon_c - \epsilon_m)}{\epsilon_m + n(1 - \phi)(\epsilon_c - \epsilon_m)} \right]$$

where ϵ_{eff} , ϵ_c , and ϵ_m are the dielectric constant of the composites, BCZT ceramic and the P(VDF-TrFE) matrix, respectively, ϕ is the volume fraction of the ceramics and n is the correction factor (ceramic morphology factor) to compensate for the shape of the fillers used in polymer ceramic composites. A small value of n

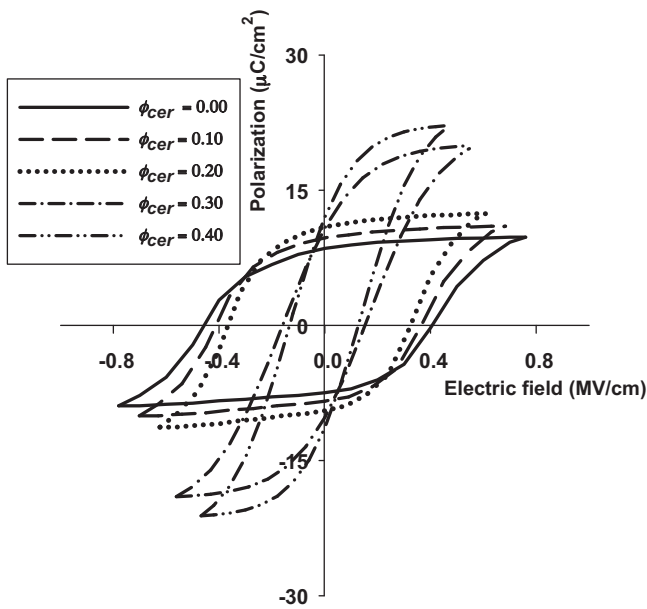


Fig. 7. Hysteresis loops of the 0–3 composites with different BCZT volume fractions measured at room temperature and 10 Hz.

indicates a near-spherical shape for the filler, while a high value of n shows a largely non-spherically shaped particle [39]. The comparison of experimental and theoretical dielectric constant calculated by EMT model at 1 kHz is shown as solid line in Fig. 6. In these calculations, the values used for ϵ_c and ϵ_m are 2800 and 11.2, respectively. For low volume contents of up to 20 vol% the measured data agrees well with the model, but at higher ceramic loading there is an increasing discrepancy between predicted and measured data. A similar observation has been reported for some polymer–ceramic composites [40,41]. This is due to the imperfect dispersing of the ceramic particles at higher filler content. It is to be noted that the morphology fitting factor obtained from the fit ($n=0.11$) is closer to the theoretically reported value ($n=0.13$) [39], and is consistent with that observed irregular shaped particles.

3.3. Ferroelectric properties

Ferroelectric polarization–electric field (P–E) loops of the 0–3 composites with different BCZT volume fractions are presented in Fig. 7. For comparison the hysteresis loop of pure copolymer sample is shown, too. The pure copolymer sample shows a well-defined square P–E loop with a remanent polarization (P_r) and coercive field (E_c) of $8.6 \mu\text{C cm}^{-2}$ and 0.41 MV cm^{-2} , respectively. These values are in good agreement with those reported in Ref. [42] for the same copolymer composition. The P–E hysteresis loops of the composites are strongly depending on the ceramic volume fraction. All composites show a higher P_{sat} than the pure copolymer, which can be attributed to the contribution of BCZT. Composites with lower ceramic volume fraction (less than 20%) show a little decrease in coercive field and obvious increase in remnant polarization. With an increase in ceramic volume fraction from 0.05 to 0.2, the remanent polarization increases from about 8.6 to $11.0 \mu\text{C cm}^{-2}$ and the coercive field decreases from 0.41 to 0.32 MV cm^{-1} . The composites with higher ceramic volume fractions showed a remanent polarization of $\sim 12 \mu\text{C cm}^{-2}$, but the coercive field reduced significantly ($\sim 0.125 \text{ MV cm}^{-1}$ for the composite with $\phi = 0.4$).

A possible reason for this behavior may be the decrease in the amount of copolymer with the increase in ceramic volume

fraction. This leads to connectivity between the ceramic particles, like to form 1–3 type composites [43]. Pardo et al. [44] reported on the hysteresis properties of mixed connectivity composites formed by the dispersion of ceramic particles into a polymer matrix, where 0–3 composites having grain sizes comparable to their thicknesses possessed a certain amount of 1–3 connectivity. It was noted by these workers that the ceramic with 1–3 connectivity will acquire a polarization value close to that of the ceramic alone under the same field, whereas, the ceramic within the 0–3 connectivity portion of the composite will experience a lower local field, because of the shielding of the polymer, and will therefore acquire a lower polarization. The amount of 1–3 connectivity will depend greatly on the ratio of ceramic grain size to composite thickness and also the ceramic volume fraction of the composite. Therefore for the composite system investigated here, the more volume fraction of ceramic, the more 1–3 connectivity is formed in the composites. That is why the remanent polarization of the composite increases and the coercive field decreases at higher volume fraction.

3.4. Mechanical properties

It is important to study the mechanical properties of the composite, as it will influence the performance of the films, e.g. for sensor and actuator applications. Mechanical measurements were performed in all BCZT/P(VDF–TrFE) composites samples and the results are summarized in Fig. 8, where the change of tensile strength, tensile strain, and Young's modulus for the composite samples are plotted against the BCZT weight fractions. The tensile strength of pure copolymer was 27.9 MPa . It increased with increasing weight fraction and reached a maximum at BCZT volume fraction of 0.2. The maximum strength was 32% higher than that of the pure copolymer. When the volume fraction was higher than 0.2, the tensile strength began to decrease. The Young's modulus increased almost linearly with an increase in BCZT content. When the ceramic volume fraction was 0.4, the Young's modulus was 2.0 GPa , which was 12% higher than that of pure copolymer. The tensile strain decreased with increasing BCZT content.

It is well known that when rigid particles are added into a polymeric matrix, the interface region formed as a result of bonding between filler and matrix can hinder crack propagation and hence provide a reinforcing effect. On the other hand, the addition of too much particulate can cause stress concentration in the regions of high particle content, which has a weakening effect on composite's properties [45,46]. When the weight loading is below 0.2 volume fraction, the reinforcing effect plays the major role. This can be due to the improved bonding between the filler and matrix through the titanate based coupling agents. Therefore, a strong interface is formed and with an increasing in the BCZT content, the deformation of the polymer matrix surrounding the particles is limited, which results in the increase of the tensile strength [47]. This type of behavior was well established in the literature [48,49]. However, when the particle fraction is more than 0.2 volume fraction the weakening effect caused by stress concentration is dominant. This is explained with respect to two aspects: (1) the strength is reduced due to the excessive proximity among particles at higher concentration and this will lead to bigger fractures from tiny cracks and (2) the increase of particles makes it more difficult for dispersion, and easier for particle “agglomeration”. Since agglomerated particles makes it possible to generate defects on the material surface, stress concentration will likely occur within the matrix, or agglomerated particles will generate slippage within the materials due to external force, resulting in a decreased tensile strength. Therefore, the tensile strength increased to a maximum at 0.2 volume fraction and then decreased with further increasing particle fraction.

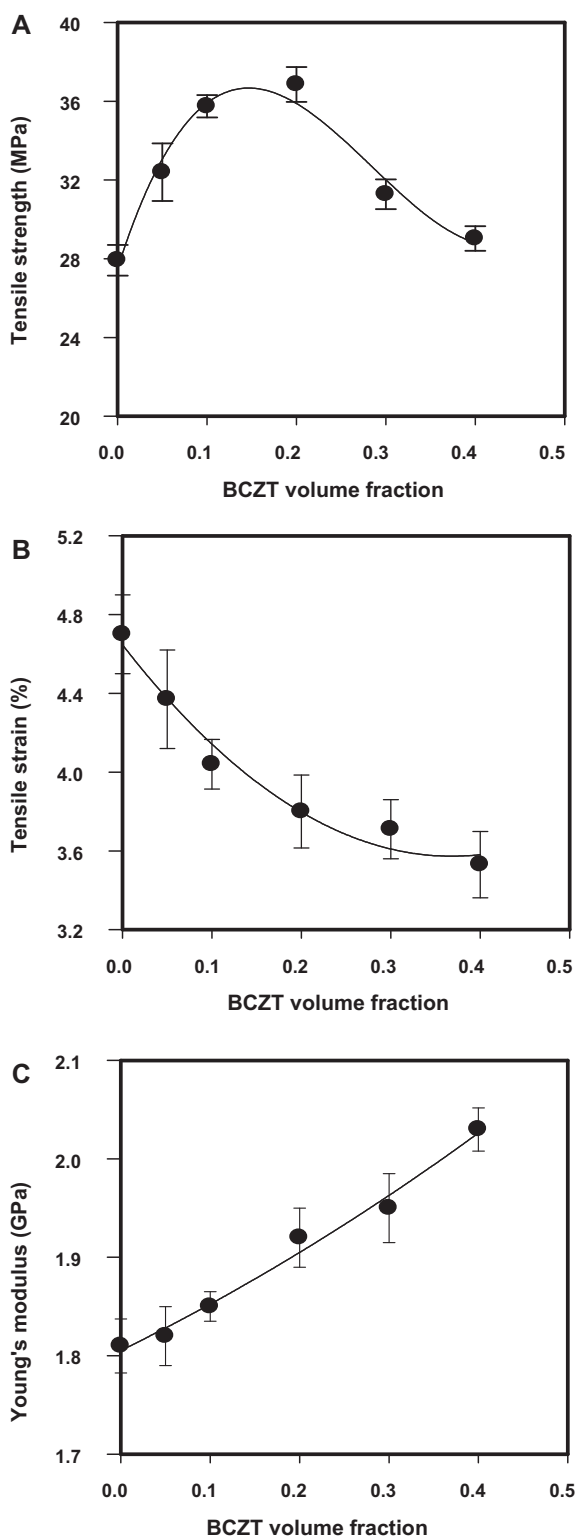


Fig. 8. Percentage change of tensile strength, tensile strain, and Young's modulus for BCTZ/P(VDF-TrFE) composites as a function of BCZT volume fraction.

The Young's modulus reflects the stiffness of a material. With increase in amount of BCZT, the particle/matrix surface area increases as does the force which the matrix material can transfer to the rigid particles. Since rigid fillers are hard to deform, the Young's modulus increases with increasing BCZT content [50].

4. Conclusions

A novel series of barium calcium zirconate titanate (BCZT) ceramic–polymer composites has been developed and characterized. The dielectric properties of these composites could be tuned by varying the volume fraction of the BCZT particles. A higher dielectric constant of up to 90 and a dielectric loss down to 0.024 could be obtained at 1 kHz for a BCZT volume fraction of 0.4. The P – E hysteresis loops of the composites are strongly dependent on the ceramic volume fraction. The composites with higher ceramic volume fractions showed larger remanent polarization and coercive field. The tensile strength increased to a maximum at 0.2 volume fraction and then decreased. With increasing BCZT volume fraction, the Young's modulus increased and the tensile strain decreased. Work is in progress to investigate the piezoelectric and pyroelectric properties of these composites.

References

- [1] K.W. Kwok, H.L.W. Chan, C.-L. Choy, *Ferroelectrics* 195 (1997) 119–122.
- [2] M. Arbatti, X.B. Shan, Z.Y. Cheng, *Adv. Mater.* 19 (2007) 1369–1372.
- [3] P. Marin-Franch, D.L. Tunnicliffe, D.K. Das-Gupta, *Mater. Res. Innov.* 4 (2001) 334–339.
- [4] M.P. Wenger, P.L. Almeida, P. Blanas, R.J. Shuford, D.K. Das-Gupta., *Polym. Eng. Sci.* 39 (1999) 483–492.
- [5] Y. Bai, Z.Y. Cheng, V. Bharti, H.S. Xu, Q.M. Zhang, *Appl. Phys. Lett.* 76 (2000) 3804–3806.
- [6] I. Vrejoiu, J.D. Pedarnig, M. Dinescu, S. Bauer-Gogonea, D. Bauerle, *Appl. Phys. A* 74 (2002) 407–409.
- [7] A. Pelaiz-Barranco, R. Lopez-Noda, *J. Appl. Phys.* 102 (2007) 114102.
- [8] A. Pelaiz-Barranco, P. Marin-Franch, *J. Appl. Phys.* 97 (2005) 034104.
- [9] S.V. Glushanin, V.Y. Topolov, *J. Phys. D: Appl. Phys.* 38 (2005) 2460–2467.
- [10] A. Seema, K.R. Dayas, J.M. Varghese, *J. Appl. Polym. Sci.* 106 (2007) 146–151.
- [11] N. Nanakorn, P. Jalupoom, N. Vaneesorn, A. Thanaboonsombut, *Ceram. Int.* 34 (2008) 779–782.
- [12] K.I. Mimura, T. Naka, T. Shimura, W. Sakamoto, T. Yogo, *Thin Solid Films* 516 (2008) 8408–8413.
- [13] S.H. Xie, B.K. Zhu, X.Z. Wei, Z.K. Xu, Y.Y. Xu, *Composites Part A* 36 (2005) 1152.
- [14] S.H. Choi, I.D. Kim, J.M. Hong, K.H. Park, S.G. Oh, *Mater. Lett.* 61 (2007) 2478.
- [15] Z.M. Dang, Y.H. Wang, Y.H. Zhang, J.Q. Qi, *Macromol. Rapid Commun.* 26 (2005) 1185.
- [16] T.A. Jain, K.Z. Fung, J. Chan, *J. Alloys Compd.* 468 (2009) 370.
- [17] Q.M. Zhang, H.F. Li, M. Poh, H.S. Xu, Z.Y. Cheng, F. Xia, C. Huang, *Nature* 419 (2002) 284.
- [18] Z.M. Dang, Y.H. Lin, C.W. Nan, *Adv. Mater.* 15 (2003) 1625.
- [19] Z.M. Dang, L. Wang, Y. Yin, Q. Zhang, Q.Q. Lei, *Adv. Mater.* 19 (2007) 852.
- [20] H.S. Nalwa, *Ferroelectric Polymers: Chemistry, Physics, and Applications*, Marcel Dekker, New York, 1995.
- [21] Q.M. Zhang, V. Bharti, X. Zhao, *Science* 280 (1998) 2101–2105.
- [22] Z.Y. Cheng, V. Bharti, T.B. Xu, H. Xu, T. Mai, Q.M. Zhang, *Sens. Actuators A* 90 (2001) 138.
- [23] Z.M. Li, M.D. Arbatti, Z.Y. Cheng, *Macromolecules* 37 (2004) 79–85.
- [24] V. Bobnar, B. Vodopivec, Z. Kutnjak, M. Kosec, A. Levstik, B. Hilczer, *Ferroelectrics* 304 (2004) 833–837.
- [25] C.K. Wong, F.G. Shin, *J. Appl. Phys.* 97 (2005) 0641111–0641119.
- [26] K.W. Kwok, C.K. Wong, R. Zheng, F.G. Shin, *Appl. Phys. A* 81 (2005) 217–222.
- [27] M. Dietze, J. Krause, C.H. Solterbeck, M. Es-Souni, *J. Appl. Phys.* 101 (2007) 054113-1–154113-7.
- [28] B. Ploss, W.Y. Ng, H.L.W. Chan, B. Ploss, C.-L. Choy, *Compos. Sci. Technol.* 61 (2001) 957–962.
- [29] K.H. Lam, H.K.W. Chan, H.S. Luo, Q.R. Yin, Z.W. Yin, C.H. Choy, *Micro. Eng.* 66 (2003) 792–797.
- [30] K.H. Lam, H.L.W. Chan, *Compos. Sci. Technol.* 65 (2005) 1107–1111.
- [31] S.T. Lau, K. Li, H.L.W. Chan, *Ferroelectrics* 304 (2004) 849–852.
- [32] A.V. Bune, V.M. Fridkin, S. Ducharme, L.M. Blinov, S.P. Palto, A.V. Sorokin, S.J. Yudin, A. Zlatkin, *Nature* 391 (1998) 874.
- [33] J. Choi, C.N. Borca, P.A. Dowben, A. Bune, M. Poulsen, S. Pebley, S. Adenwalla, S. Ducharme, L. Robertson, V.M. Fridkin, S.P. Palto, N.N. Petukhova, S.G. Yudin, *Phys. Rev. B* 61 (2000) 5760.
- [34] W. Li, Z. Xu, R. Chu, P. Fu, G. Zang, *Mater. Lett.* 64 (2010) 2325–2327.
- [35] C. Muralidhar, P.K.C. Pillai, *J. Mater. Sci.* 23 (1998) 1071.
- [36] X.X. Wang, K.H. Lam, X.G. Tang, H.L.W. Chan, *Solid State Commun.* 130 (2004) 695–699.
- [37] M.T. Sebastian, H. Jantunen, *Rev. Int. J. Appl. Ceram. Technol.* 7 (2010) 415–434.
- [38] Y.C. Rao, C.P. Wong, J. Qu, T. Marinis, *IEEE Trans. Comp. Packag. Technol.* 23 (2000) 680–683.
- [39] M.G. Todd, G.F. Shi, *Micro. J.* 33 (2002) 627–632.

- [40] S. Thomas, V. Deepu, P. Mohanan, M.T. Sebastian, *J. Am. Ceram. Soc.* 91 (2008) 1970–1975.
- [41] V.S. Nisa, S. Rajesh, K.P. Murali, V. Priyadarsini, S.N. Potty, R. Ratheesh, *Comp. Sci. Technol.* 68 (2007) 106–111.
- [42] R. Kohler, N. Neumann, G. Hofmann, *Actuator A* 45 (2004) 209–218.
- [43] C.J. Dias, D.F. Das-Gupta, *IEEE Trans. Dielectr. Electr. Insul.* 3 (1996) 709.
- [44] L. Pardo, J. Mendiola, C. Alemany, *J. Appl. Phys.* 64 (1988) 5092.
- [45] N.C. Bleach, S.N. Nazhat, K.E. Tanner, M. Kellomaki, P. Tormala, *Biomaterials* 23 (2002) 1579–1585.
- [46] S. Debnath, R. Ranade, S.L. Wunder, J. McCool, K. Boberick, G. Baran, *Dent. Mater.* 20 (2004) 677–686.
- [47] G. Gong, B.H. Xie, M.B. Yang, W. Yang, W.Q. Zhang, M. Zhao, *Composites Part A* 38 (2007) 1683–1693.
- [48] M. Hashimoto, H. Takadama, M. Mizuno, T. Kokubo, *Mater. Res. Bull.* 41 (2006) 515–524.
- [49] Y. Rong, H.Z. Chen, G. Wu, M. Wang, *Mater. Chem. Phys.* 91 (2005) 370–374.
- [50] S.Y. Fu, X.Q. Feng, B. Lauke, Y.W. Mai, *Composites Part B* 39 (2008) 933–961.